

8054

ЭНЕРГИЯ

ОБЪЕДИНЕННЫЙ
ИНСТИТУТ
ЯДЕРНЫХ
ИССЛЕДОВАНИЙ

ДУБНА



E1 - 8054

**A.M.Baldin, N.Ghiordanescu, L.K.Ivanova,
N.S.Moroz, A.A.Povtorejko, V.B.Radomanov,
V.S.Stavinsky, V.N.Zubarev**

**AN EXPERIMENTAL INVESTIGATION
OF CUMULATIVE MESON PRODUCTION**

1974

ЛАБОРАТОРИЯ ВЫСОКИХ ЭНЕРГИЙ

E1 - 8054

A.M.Baldin, N.Ghiordanescu, L.K.Ivanova,
N.S.Moroz, A.A.Povtorejko, V.B.Radomanov,
V.S.Stavinsky, V.N.Zubarev

**AN EXPERIMENTAL INVESTIGATION
OF CUMULATIVE MESON PRODUCTION**

Submitted to ЯФ

**Научно-техническая
библиотека
ОИЯИ**

Балдин А.М., Гиордэнеску Н., Иванова Л.К.,
Мороз Н.С., Повторейко А.А., Радоманов В.Б.,
Ставинский В.С., Зубарев В.Н.

E1 - 8054

Экспериментальные исследования кумулятивного
мезообразования

В работе измерены энергетические спектры мезонов, образованных на ядрах D, C, Al, Cu, Pb протонами с импульсом 6 и 8,4 ГэВ/с под углом 180°. Наблюдавшийся кумулятивный эффект до четвертого порядка включительно описывается простыми закономерностями.

Препринт Объединенного института ядерных исследований.
Дубна, 1974

Baldin A.M., Ghiordanescu N., Ivanova L.K.,
Moroz N.S., Povtorejko A.A., Radomanov V.B.,
Stavinsky V.S., Zubarev V.N.

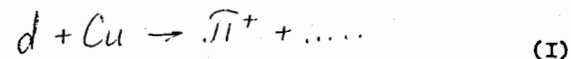
E1 - 8054

An Experimental Investigation of Cumulative
Meson Production

The energy spectra of mesons, produced on nuclei D, C, Al, Cu, Pb by 6 and 8.4 GeV/c protons at an angle of 180°, have been measured. It is shown that in the antilaboratory system these reactions correspond to the processes of the interaction of relativistic nuclei with protons. As a result, the produced mesons take the energy much higher than that per one nucleon of a relativistic nucleus. The observed cumulative effect to the 4th order inclusive is described by simple regularities.

Preprint. Joint Institute for Nuclear Research.
Dubna, 1974

A study^{/1,2/} of the energy spectrum of particles in the reaction



has led to discovery of the meson production effect for three-nucleon collisions. According to estimates^{/3,4/}, this effect turned out to be so significant that it is accessible not only to experimental study but also it can be of practical importance. The same estimates^{/3,4/} show that the cumulative meson production processes of higher order cumulativity must have sufficiently large cross sections. The reaction of a relativistic nucleus and a target one, in which the new produced particle has an energy substantially exceeding that per one nucleon of an incident nucleus, is called cumulative effect.

As a cumulative order we understand the number of nucleons of the incident relativistic nucleus participating in the collision. It is natural that such a definition raises a question on the separation of the cumulative effect from those which are due to the Fermi-motion of nucleons inside the bombarding nucleus.

For definiteness, as bounds on an energy scale of secondary particles between the cumulative effects of neighbouring order, we indicate maximal energies of secondaries for previous order particles without taking into account the Fermi motion. This definition becomes more and more accurate with increasing the energy of the relativistic nucleus. It implies smallness (in any case finiteness) of the momentum of nucleon internal motion in comparison with that of one nucleon of the relativistic nucleus.

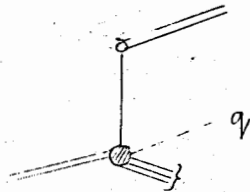
In fact, the cumulative effect is separated more accurately on the basis of the scale invariance and asymptotic properties of the matrix elements.

The concept of compound particle is usually defined by the result of decomposition of its state into the constituent states. For example, the nucleus state with mass number A is described to a good approximation by one term of expansion in the number of constituents:

$$|A\rangle = \sum_N |N\rangle \langle N|A\rangle \approx |N_0\rangle \langle N_0|A\rangle$$

$$|\langle N_0|A\rangle|^2 \approx 1,$$

where $|N_0\rangle$ is the state describing A nucleons. The states, in which mesons, hyperons, isobars, etc., are present, are assumed to make a negligible contribution. This basic postulate of nuclear physics is supported by a great number of experimental data. If the state is written in momentum representation, the corresponding amplitude will define the probability of finding particular momentum values. This is a definition of the Fermi motion of nucleons inside nuclei. One can draw a conclusion about the role of this motion without detailing the wave function models of nuclei. When the influence of the Fermi motion is talked about, the above mechanism is determined by the following diagram:



The corresponding matrix element takes the form

$$\frac{\Gamma(p^2)}{p^2 - m^2} M(p^2, \xi),$$

where P_A and P_A' are 4-momenta of incident and residual nuclei, P is the nucleon momentum which induces the meson production with momentum q ; ξ are all other variables including q .

The case $|\vec{q}|^2 \sim |\vec{P}_A|^2 \gg M_A^2$ is of our interest (imitation of the cumulative effect), where $P^2 = (P_A - P_A')^2 = -2E_A M_A^{-1} S$. According to the theorem of Lehmann, Symanzik and Zimmermann, the vertex part Γ decreases at $P^2 \rightarrow \infty$. One can see that the part of the invariant cross section $2E d^3G/d\vec{p}$ which is due to the Fermi motion has no a scale invariance property and decreases with increasing E_A faster than $1/E^2$ (or $1/S^2$) does.

Based on this consideration we can give a method of separation of the cumulative effect from those of Fermi motion: it is necessary the invariant cross section $R_A = 2E \frac{d^3G}{d\vec{p}}$ should be expanded in a power series ($1/S$); a zero term of this series separates the N -th order of the cumulative effect at $q_{N-1}^{\max} \leq q \leq q_N^{\max}$, where q_N^{\max} is the momentum of secondary particle and q_N^{\max} is its maximum value for the collision of N -nucleons inside the relativistic nucleus.

Paper^{/I/} shows that for reaction (I) such a zero term exists, scale invariance being fulfilled. Calculations in the impulse approximation^{/2,10/} which are in agreement with the above argumentation indicate that the observed effect cannot be explained by the Fermi motion of nucleons inside deuterium and copper nuclei. It is also shown in the experiment^{/1,2/} that the ratio between the invariant functions $R_A = 2E \frac{d^3G}{d\vec{p}}$ of deuterons and protons at equal values of the scale argument $x = p_{\pi} / p_{\pi}^{\max}$ (for $x > 0.5$), within errors, is independent of the argument x and is equal to

0.06. The latter is in agreement with the simplest model of cumulative meson production^{/2,3/}. According to this model, finding and investigation of different characteristics of this process turn out to be quite real. The dependence of the secondary particle yield on the atomic number of the relativistic nucleus is an important and, for the present, unstudied characteristic of the cumulative effect. Investigations of scale invariance effects and finding of, as high as possible, cumulative orders are problems of today.

This paper is devoted to solving these problems. Below we present and discuss the experimental data on the reactions $A + p \rightarrow \pi^\pm (K^+) + \dots$ (2) obtained in the coordinate system, where nucleus A is at rest, and mesons are detected at an angle of 180° . This statement of the problem makes it possible to get information of our interest before we study the beams of relativistic nuclei with $A \gg 4$ at the energy permitting one to separate the cumulative effect from those which are due to Fermi motion. The problem of relativistic acceleration of mean-weight nuclei and, possibly, of heavy ones is likely to be solved only after creating a specialized accelerator of relativistic particle - Nuclotron^{/9/}.

In reaction (2) D, C, Al, Cu, Pb were taken as nuclei A. Reaction (2) was studied with momenta 6 and 8.4 GeV. The energy of secondary mesons varied from 100 to 1070 MeV. This corresponds to discovery of the cumulative effect up to the 4th order inclusive (as many as 4 nucleons out of A take part in the collision). As will be seen below, the invariant cross sections $R_A = 2E \frac{d^3N}{d^3p}$

are weakly dependent on β in the whole of the energy range studied. As will be shown later on, the energy spectrum of produced pions is described by the following simple exponential dependence

$$R_A = R_A^{(0)} \exp \left\{ -T/T_0 \right\},$$

where the parameter T_0 is practically independent of energy. The ratio

$$\frac{R_A^{(0)}(6) - R_A^{(0)}(8.4)}{R_A^{(0)}(6)}$$

for the carbon target is equal to -0.2 ± 0.1 , i.e., within the accuracy of our measurements, the contribution of the terms of higher order than zero one in expansion R_A in a power series $(\frac{1}{3})$ is practically absent. According to the above argumentation, it means that at our energies the influence of Fermi motion is negligible and only the cumulative effect is observed. Thus, the data presented below show that the cumulative effect is found up to the 4th order and permits one to check the models of cumulative meson production.

The experimental layout is shown in fig. 1. The primary beam was monitored by a scintillation telescope M. Pions were detected by three scintillation counters S_1, S_2, S_3 and a Cherenkov counter C in coincidence ($N_{\pi} = S_1 + S_2 + S_3 + C$). The spectrometer has the momentum acceptance $\Delta p/p = 6\%$ and the angular acceptance less than 30 mrd for emission angle $\langle \theta \rangle = 180^\circ$. Thus, the maximum transverse momentum of detected mesons was

not larger than 30 MeV/c. The detecting apparatus is described in more detail in ref.^{/5/}. It should be noted that the proposed method of measuring the spectra of secondary particles for the nucleon-nucleon interaction in the range of small momentum transfers (t) is a more accurate one for measuring the t -dependence at ultrarelativistic energies.

Calculation of Meson Production Cross Sections

We shall present the experimental data in the invariant production cross section

$$\sigma_A = 2 E_{\pi} d^3\sigma/dp^3$$

or inclusive density

$$\rho = \frac{2 E_{\pi}}{\sigma_{t+t}} \frac{d^3\sigma}{dp^3}.$$

The function R_A is expressed as follows:

$$R_A = \frac{2 E_{\pi}}{P_{\pi}^2} \frac{1}{P_K S_K} \frac{K}{\epsilon_A} h \left[\int_{S_A} \frac{N_{\pi}(A)}{M_P(A)} - \frac{N_{\pi}(\Pi)}{M_P(\Pi)} \right] \quad (4)$$

where E_{π} , P_{π} are the total energy and momentum of secondary mesons; the product $P_K S_K = \Delta \Omega \Delta P$, where $\Delta \Omega$ is the transmission solid angle of the spectrometer and ΔP is the acceptance of the momenta^{/5/}. The constant K takes into account the correction for absorption in the matter of the counter and the target, pion disintegration and muon contamination. The constant h connects the monitor counts in measurements without target ($M(\Pi)$) with the primary beam intensity. The monitor was calibrated absolutely by measuring C^{12} activity. The constant ξ ($\xi \approx 1.02 + 1.10$) takes into account the change of monitor count ($M_P(A)$) when the target (A) is placed into the beam; $N_{\pi}(A)$

are meson counts from the target A (l_A in thickness) expressed in inverse millibarns and $N_{\pi}(\Pi)$ are counts without target.

The systematic error in measuring R_A is due to uncertainty in constants P_K , S_K , K and h .

The momentum of detected particles P_K is determined by the graduated curve obtained by a floating wire technique^{/5/}. The systematic error in graduations is 3%.

The constant S_K was computed using a standard program^{/5/}. For the given geometry of the experiment, the systematic error in determining S_K is 8%.

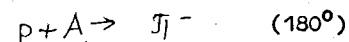
The systematic error in calculating the constant K is mainly due to meson decay. This correction is maximum for small meson momenta. For example, for the momentum of secondary mesons 200 MeV/c it is equal to 1.5, and its uncertainty is 3% and 1% for large values of P_K .

The systematic error in calibration with the activity produced in the CH target is determined by uncertainty in the cross section of reaction $C^{12}(p, np)C^{11}$ and is equal to 6%.

Thus, the total systematic error in measuring R_A (if all indicated factors are independent) is about 10%.

Experimental Data

Table I presents the experimental data on the invariant cross section (R_A) of the inclusive process



when nuclei C, Al, Cu and Pb are excited by 6.0 GeV/c protons.

The errors presented are statistical. The kinetic energy of nega-

tive pions varied from 109 to 673 MeV. According to the kinematics of the nucleon-nucleon interaction

$$N + N \rightarrow \pi^- (180^\circ).$$

The energy of secondary pions must not exceed $T_{\max} = 244$ MeV. Thus, according to our definition (see above), the majority of our experimental data corresponds to cumulative meson production.

Figures 2, 3, 4 present the experimental data on the invariant cross sections $dE \frac{d^3s}{dp^3}$ for nuclei C, Al and Cu as a function of the kinetic energy of negative pions. One can see from the figures that the dependence of the cross sections on the pion kinetic energy is of an exponential character, the spectra of various nuclei being similar and, in a first approximation, differing in constant.

Table II shows the experimental data on the invariant cross sections of the positive meson production on nuclei C, Al, Cu and Pb excited by 8.4 GeV/c protons. The energy of generated pions varies from 115 to 676 MeV. The kinematic limit for the nucleon-nucleon interaction is 269 MeV. Thus, again the greater part of experimental data on the positive pion production corresponds to collective multinucleon interactions inside the target-nucleus.

In figs. 5, 6, 7, 8 one can see the experimental data on the pion production (π^+) on target-nuclei C, Al, Cu and Pb. As is seen from the figures, the energy spectra of pions are of an exponential character and similar for various nuclei.

For comparison figure 5 presents the energy spectrum of protons (p^+) for the carbon target^{6/} exposed to 6.6 GeV/c protons.

From this comparison one concludes that the invariant cross section of pions can be compared with that of protons as a function of the kinetic energy of produced particles. However, the "temperature" of the proton spectrum is somewhat lower than that of the meson one.

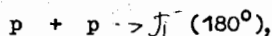
In figs. 5 and 7 one can see the preliminary data on the invariant yield of positive kaons for carbon and copper nuclei. It is seen from the figures that at equal kinetic energies of the produced mesons, the kaon yield is approximately two orders less than the meson one. The kinematic limit of kaon production in the nucleon-nucleon interaction is equal to ~ 40 MeV. Consequently, the observed kaons have an energy ($T_L = 200 - 300$ MeV) which is significantly higher than the kinematic limit for the nucleon-nucleon interaction and corresponds to the 3rd order cumulative effect.

In Table III we present the experimental data on the invariant cross sections of the negative pion production when nuclei C, Al, Cu and Pb are excited by protons with momentum 8.4 GeV/c. The kinetic energy of created pions varied from 119 to 1072 MeV. The kinematic limit corresponds to the nucleon-nucleon interaction equal to 269 MeV.

As an illustrative example, these data are presented in figs. 9, 10, 11, 12. It is seen that if the energies of produced pions are lower than 700 MeV, the energy spectra, as before, are of an exponential character and similar for various nuclei. However, if the energies of produced pions are high, a deviation from the exponential dependence is observed. According to our definition, the observed pions correspond to the observation of the 4th order

cumulative effect. Although the errors of measurement are large (50%) in this range of energy spectrum, the deviation from the exponential dependence is observed for all the investigated nuclei. (Possible systematic errors have been tested experimentally as follows. For pions at 1072 MeV (copper-target) the angular resolution of the Cherenkov counter (and the energy resolution connected with them) was decreased by a factor of 3 to the angular acceptance of particles in the channel. The effect, within errors, remained previous. Using an absorber (Fe, 20 cm) located in front of the counter S_3 (fig. 1) it was shown that detected particles could not be muons with momentum larger than 400 MeV/c.

In Table IV we present the experimental data on the invariant cross section of the negative pion production $\rho = \frac{2E}{\sigma_{tot}} \frac{d^3\sigma}{dp^3}$ for the reaction



measured by the subtraction method CH_2-C , and the experimental data on the reaction



obtained by the subtraction method CD_2-C . The same Table shows the experimental data on the reaction $N_{Cu} + d \rightarrow \pi^-$ obtained earlier^{4/}.

Empirical Regularities

A similarity of the energy spectra, their exponential character permit one to describe the function $2E \frac{d^3\sigma}{dp^3}$ by a simple exponential dependence and to analyse the parameters. The experimental values $2E \frac{d^3\sigma}{dp^3}$ were fitted to the following functions:

and

$$2E \frac{d^3\sigma}{dp^3} = a_1 \exp\left\{-T/T_0\right\} + a_2 \quad (\text{fit 1})$$

$$2E \frac{d^3\sigma}{dp^3} = a_1 \exp\left\{-T/T_0\right\}. \quad (\text{fit 2})$$

According to the criterion χ^2 , the experimental data are well described by the exponential functions (Maxwell distribution).

Table V presents the distribution parameters and their errors. It is seen from the Table that the parameter T_0 ("temperature") is practically independent of the energy of primary protons and the charge sign of secondary mesons. The parameter a_1 is also independent of the charge of secondary mesons and weakly changes with the energy of primary protons. One can see from Table V that a_1 practically linearly increases with increasing the atomic number of target-nucleus. Figure 13 shows the experimental data on the production of negative pions by 8.40 GeV/c protons as a function of the atomic number of target-nucleus for various kinetic energies of produced pions. The linear dependence on the atomic number A is plotted in the same figure (dotted line). The experimental data for various pion energies were fitted to the following relation

$$2E \frac{d^3\sigma}{dp^3}(T_{\pi}) = R_1(T_{\pi}) A^n(x),$$

where $x = T_{\pi}/T_{\pi}^{max}$ and T_{π}^{max} is the maximum kinetic energy of pion for the nucleon-nucleon interaction kinematics. Figure 14 shows the parameter n versus the variable x . The values of parameter a_1 are used to find the parameter n in the point

$\chi = 0$ (fit 1) (Table V). From fig. 14 it is seen that at $\chi = T_{\pi}/T_{\pi}^{\text{MAX}}$ the parameter n does not depend on the primary energy of protons and the charge sign of generated pions. If the energy of produced pions approaches 0, the parameter n tends to $2/3$. With increasing the pion energy up to T^{MAX} , the parameter n increases achieving unit at $\chi = 1$. In the range of cumulative meson production ($\chi > 1$) the parameter n , within errors, remains constant at the level of unit. Such a behaviour of the parameter n indicates that in the range of ordinary (noncumulative) meson production ($\chi < 1$) the cross section of particle production is proportional to the nuclear surface ($n \sim 2/3$), and in the region of cumulative meson production ($\chi > 1$) the cross section of meson creation is proportional to the nucleus volume ($n \sim 1$).

Thus, the studied process, fragmentation process of target-nucleus (A), excited by protons at 6 and 8.4 GeV/c has the following empirical regularities:

1) The energy spectrum of produced pions in the coordinate system, related to the nucleus, is of an exponential character

$$2E \frac{d^3 \tilde{\sigma}}{dP^3} \sim a_A \exp\left\{-T/T_0\right\}$$

parameters a_A and T_0 being practically independent of the energy of primary protons. Thus, the pion spectra for nuclei C, Al, Cu, Pb satisfy the scale invariance requirement (at least, for a high energy part of the pion spectrum ($T > m_{\pi}$)) found earlier for deuterium nuclei^{/3,4/}. This indicates that the Fermi motion effects are unessential.

2) The coefficient a_A depends on the atomic number of target nucleus ($a_A \sim a_0 A^k$), the index n being dependent on the energy of produced pions. At low pion energies ($T \sim 0$) we have $n(T \sim 0) \approx 2/3$. In the range of cumulative meson production ($\chi \gg 1$) $n \approx 1$. A strong dependence of the meson production cross section on the atomic number A shows that it is possible to obtain intensive beams of cumulatively produced particles for accelerated^{/7,8,9/} relativistic nuclei

$$Atp \rightarrow (p, \kappa, \tilde{\pi})$$

Figure 15 presents the spectra $d^2 \tilde{\sigma}/dP d\Omega$ of cumulative mesons ($\tilde{\pi}$) for carbon and copper nuclei with momenta 6 (†) and 8.4 (‡) GeV/c per nucleon (this paper) and the spectrum of cumulative protons (dotted curve)^{/6/}. One can see that the yield of protons significantly exceeds (approximately by a factor of 10^4) that of pions at equal momenta of secondary particles. Possibly, this is an evidence for an essentially different nature of these processes. However, it should be noted that

$$\frac{d^2 \tilde{\sigma}_{\tilde{\pi}}}{dP d\Omega}(P_{\tilde{\pi}}) \approx \frac{d^2 \tilde{\sigma}_P}{dP d\Omega}(P_P - P_0),$$

where P_0 is the momentum per one nucleon of accelerated nucleus. It is also seen from the figure that the yield of kaons for carbon (★) and copper (☆) nuclei coincides with that of pions. Thus, the expression

$$\frac{d^2 \tilde{\sigma}_K}{dP d\Omega}(P_P - P_0) \approx \frac{d^2 \tilde{\sigma}_{K^+}}{dP d\Omega}(P_{K^+}) \approx \frac{d^2 \tilde{\sigma}_{\tilde{\pi}^+}}{dP d\Omega}(P_{\tilde{\pi}^+})$$

is probably valid for any nucleus accelerated to equal momenta per one nucleon.

A more detailed discussion of data, in particular their comparison with the cumulative model, will be presented elsewhere.

In conclusion we would like to express our gratitude to chief engineer L.G.Makarov, a synchrotron crew under the guidance of S.V.Fedukov, to I.B.Issinsky, A.A.Smirnov and K.V.Chekhlov and their colleagues for stable operation of the accelerator during the experiment. We express our acknowledgement to V.G.Perevozchikov and a group of A.D.Kirillov for their help in this work.

Table I

$R_A = Z^2 E \frac{d^2\sigma}{dp^2} / mb \text{ GeV}^2 c^2, pA \rightarrow \pi^-(180^\circ), 6. \text{ GeV}/c$				
$T, \text{ MeV}$	R_C	R_{AL}	R_{Cu}	R_{Pb}
109	$(3.98 \pm 0.39) 10^1$	$(8.41 \pm 0.74) 10^1$	$(1.80 \pm 0.18) 10^2$	
113	$(3.51 \pm 0.44) 10^1$			
140	$(1.82 \pm 0.19) 10^1$	$(3.96 \pm 0.37) 10^1$	$(8.48 \pm 0.88) 10^1$	
160	$(1.49 \pm 0.13) 10^1$	$(3.21 \pm 0.27) 10^1$	$(5.63 \pm 0.58) 10^1$	
185	$(1.04 \pm 0.1) 10^1$	$(2.17 \pm 0.1) 10^1$	$(4.64 \pm 0.45) 10^1$	
226	$(4.05 \pm 0.38) 10^0$	$(9.9 \pm 0.75) 10^0$	$(2.44 \pm 0.19) 10^1$	
258	$(1.89 \pm 0.28) 10^1$	$(4.95 \pm 0.59) 10^1$	$(1.37 \pm 0.17) 10^1$	
281	$(1.16 \pm 0.24) 10^1$	$(3.06 \pm 0.44) 10^1$	$(7.62 \pm 0.44) 10^0$	
302	$(1.04 \pm 0.44) 10^0$	$(2.92 \pm 0.29) 10^0$	$(5.47 \pm 0.73) 10^0$	
329	$(6.05 \pm 1.05) 10^0$	$(1.63 \pm 0.19) 10^0$	$(3.60 \pm 0.57) 10^0$	
351	$(5.30 \pm 0.88) 10^0$	$(1.44 \pm 0.15) 10^0$	$(2.91 \pm 0.46) 10^0$	
390	$(2.22 \pm 0.62) 10^1$	$(4.67 \pm 1.2) 10^1$	$(1.00 \pm 0.10) 10^0$	
477	$(2.81 \pm 1.43) 10^{-2}$	$(6.94 \pm 4) 10^{-2}$	$(3.41 \pm 0.97) 10^1$	$(8.50 \pm 4.20) 10^0$
538	$(2.42 \pm 0.93) 10^1$	$(4.74 \pm 1.34) 10^1$	$(8.36 \pm 3.72) 10^0$	
629	$(1 \pm 0.7) 10^{-2}$	$(3.30 \pm 1.74) 10^1$	$(1.04 \pm 0.50) 10^1$	
673	$(6.05 \pm 4.5) 10^{-2}$	$(1.70 \pm 1.27) 10^1$	$(6.34 \pm 2.70) 10^0$	$(1.4 \pm 0.7) 10^0$

Table II

$R_A = Z^2 E \frac{d^2\sigma}{dp^2} / mb \text{ GeV}^2 c^2, pA \rightarrow \pi^-(180^\circ), 8.4 \text{ GeV}/c$				
$T, \text{ MeV}$	R_C	R_{AL}	R_{Cu}	R_{Pb}
115	$(4.73 \pm 0.27) 10^1$	$(9.71 \pm 0.45) 10^1$	$(2.04 \pm 0.1) 10^2$	$(4.67 \pm 0.39) 10^2$
163	$(1.74 \pm 0.09) 10^1$	$(3.33 \pm 0.19) 10^1$	$(7.47 \pm 0.44) 10^1$	$(1.86 \pm 0.12) 10^2$
219	$(8 \pm 0.28) 10^0$	$(1.60 \pm 0.08) 10^1$	$(3.58 \pm 0.16) 10^1$	$(8.46 \pm 0.58) 10^1$
259	$(4.29 \pm 0.19) 10^0$	$(9.90 \pm 0.5) 10^0$	$(2.34 \pm 0.12) 10^1$	$(7.45 \pm 0.51) 10^1$
300	$(1.13 \pm 0.15) 10^0$	$(2.92 \pm 0.23) 10^0$	$(7.87 \pm 0.75) 10^0$	$(1.71 \pm 0.26) 10^1$
340	$(6.09 \pm 0.79) 10^1$	$(1.71 \pm 0.18) 10^0$	$(3.74 \pm 0.45) 10^1$	$(1.08 \pm 0.18) 10^1$
373	$(4.40 \pm 0.44) 10^1$	$(1.10 \pm 0.11) 10^0$	$(2.93 \pm 0.25) 10^1$	$(8.82 \pm 1) 10^0$
424	$(1.89 \pm 0.24) 10^1$	$(4.27 \pm 0.5) 10^1$	$(1.33 \pm 0.12) 10^0$	$(3.80 \pm 0.51) 10^0$
480	$(3.75 \pm 0.9) 10^{-2}$	$(7.15 \pm 1.88) 10^1$	$(4.54 \pm 0.63) 10^1$	$(8.31 \pm 0.24) 10^1$
676	$(1.09 \pm 0.5) 10^{-2}$	$(2.88 \pm 1.72) 10^1$	$(7.66 \pm 3.1) 10^1$	$(1.52 \pm 0.17) 10^1$

Table III

$R_A = Z^2 E \frac{d^2\sigma}{dp^2} / mb \text{ GeV}^2 c^2, pA \rightarrow \pi^-(180^\circ), 8.4 \text{ GeV}/c$				
$T, \text{ MeV}$	R_C	R_{AL}	R_{Cu}	R_{Pb}
119	$(1.85 \pm 0.19) 10^1$	$(1.12 \pm 0.09) 10^2$	$(2.13 \pm 0.17) 10^2$	$(5.28 \pm 0.8) 10^2$
168	$(1.67 \pm 0.1) 10^1$	$(3.8 \pm 0.27) 10^1$	$(8.59 \pm 0.62) 10^1$	$(1.85 \pm 0.21) 10^2$
212	$(9.34 \pm 0.98) 10^0$			
225	$(6.68 \pm 0.44) 10^0$	$(1.44 \pm 0.08) 10^1$	$(3.18 \pm 0.18) 10^1$	$(3.5 \pm 0.7) 10^1$
252	$(4.95 \pm 0.5) 10^0$			
265	$(3.26 \pm 0.12) 10^1$	$(8.38 \pm 0.48) 10^0$	$(1.85 \pm 0.14) 10^1$	$(5.65 \pm 0.8) 10^1$
283	$(2.74 \pm 0.28) 10^0$			
301	$(1.65 \pm 0.07) 10^1$	$(4.21 \pm 0.32) 10^0$	$(1.02 \pm 0.08) 10^1$	$(3.05 \pm 0.54) 10^1$
322	$(1.25 \pm 0.13) 10^0$			
331	$(1.24 \pm 0.15) 10^0$			
341	$(8.72 \pm 0.46) 10^0$	$(2.84 \pm 0.18) 10^0$	$(6.37 \pm 0.38) 10^0$	$(1.87 \pm 0.21) 10^1$
366	$(5.59 \pm 0.58) 10^0$			
379	$(4.67 \pm 0.4) 10^0$			
423	$(2.46 \pm 0.22) 10^1$	$(5.5 \pm 0.78) 10^1$	$(1.37 \pm 0.14) 10^0$	$(3.57 \pm 0.57) 10^0$
479	$(9.41 \pm 1.1) 10^{-2}$	$(2.04 \pm 0.3) 10^1$	$(5.55 \pm 0.8) 10^1$	$(1.82 \pm 0.4) 10^0$
578	$(2.33 \pm 0.58) 10^1$	$(3.84 \pm 0.78) 10^1$	$(1.44 \pm 0.26) 10^1$	$(3.54 \pm 0.12) 10^1$
676	$(8.26 \pm 2.53) 10^0$	$(2.04 \pm 0.17) 10^1$	$(4.62 \pm 0.41) 10^2$	$(1.65 \pm 0.44) 10^1$
874	$(1.95 \pm 1.43) 10^{-3}$	$(2.32 \pm 1.72) 10^1$	$(2.04 \pm 0.78) 10^1$	$(3.19 \pm 3.58) 10^1$
1072	$(1.98 \pm 1.45) 10^{-3}$	$(6.97 \pm 3.1) 10^1$	$(1.52 \pm 0.58) 10^1$	$(1.84 \pm 2.84) 10^2$

Table IV

P_p (GeV/c)	T_π (GeV)	T_π/T_{MAX}	$P \cdot \frac{2E}{\Omega p} \frac{d^2\sigma}{d\Omega dp} (p \cdot D - \sqrt{s_{180}}) (\text{GeV}^2 \cdot \text{c}^3)$
8.4	0.119	0.193	$(1.18 \pm 0.18) 10^{-1}$
8.4	0.173	0.280	$(4.1 \pm 1.1) 10^{-2}$
8.4	0.267	0.431	$(4.4 \pm 1.0) 10^{-3}$
8.4	0.304	0.491	$(2.13 \pm 0.6) 10^{-3}$
8.4	0.342	0.552	$(7.9 \pm 2.1) 10^{-4}$
6	0.110	0.197	$(8.4 \pm 2.2) 10^{-2}$
6	0.394	0.706	$(3.2 \pm 1.3) 10^{-4}$
≈ 4.7	0.289	0.573	$(1.55 \pm 0.38) 10^{-3}$
≈ 4.82	0.318	0.624	$(8.52 \pm 1.5) 10^{-4}$
≈ 5.15	0.322	0.613	$(5.9 \pm 1.3) 10^{-4}$
≈ 3.53	0.313	0.728	$(3.67 \pm 0.9) 10^{-4}$
P_p (GeV/c)	T_π (GeV)	T_π/T_{MAX}	$P \cdot \frac{2E}{\Omega p} \frac{d^2\sigma}{d\Omega dp} (p \cdot D - \sqrt{s_{180}}) (\text{GeV}^2 \cdot \text{c}^3)$
8.4	0.119	0.443	$(7.1 \pm 1.5) 10^{-2}$

Table V

TARGET	8.4 GeV/c, PA- $\pi(180^\circ)$				6.0 GeV/c, PA- $\pi(180^\circ)$				8.4 GeV/c, PA- $\pi(80^\circ)$			
	C	Al	Cu	Pb	C	Al	C	Pb	C	Al	C	Pb
X^2	11	1.7	0.9	0.9	0.82	0.75	0.73	-	5.3	7.0	4.0	5.7
Ω_i	35.6 ± 1.9	6.95 ± 0.6	2.9 ± 0.3	2.9 ± 0.3	3.3 ± 0.3	2.59 ± 0.1	0.7 ± 0.08	-	388 ± 26	74.3 ± 4.3	29.2 ± 2.0	27.92 ± 2.29
T (MeV)	5.6 ± 0.6	5.96 ± 1.0	6.24 ± 1.0	6.4 ± 1.5	5.3 ± 1.4	5.58 ± 2.5	5.83 ± 1.6	-	5.51 ± 0.9	5.58 ± 0.8	6.07 ± 1.0	6.27 ± 1.3
$\Omega_i \cdot 10^3$	128 ± 0.29	20 ± 2.1	16.7 ± 0.44	5.2 ± 2.0	1.3 ± 0.4	1.37 ± 0.6	1.0 ± 0.21	-	0.78 ± 0.03	0.14	4.8 ± 3.0	0.15
X^2	1.3	1.9	1.2	1.0	1.0	0.93	0.93	-	5.9	7.5	4.4	6.0
Ω_i	35.4 ± 1.9	6.81 ± 0.54	2.61 ± 0.97	2.8 ± 0.3	2.83 ± 0.35	2.5 ± 0.46	0.95 ± 0.13	-	383 ± 25	74.5 ± 4.3	26.1 ± 2.3	27.97 ± 2.29
T (MeV)	5.67 ± 0.6	5.98 ± 1.0	6.28 ± 1.0	6.4 ± 1.5	5.3 ± 1.4	5.56 ± 2.5	5.85 ± 1.4	-	5.52 ± 0.9	5.58 ± 0.9	6.1 ± 1.0	6.26 ± 1.3

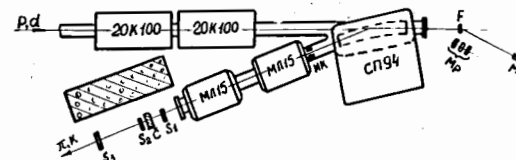


Fig. 1. Experimental layout.

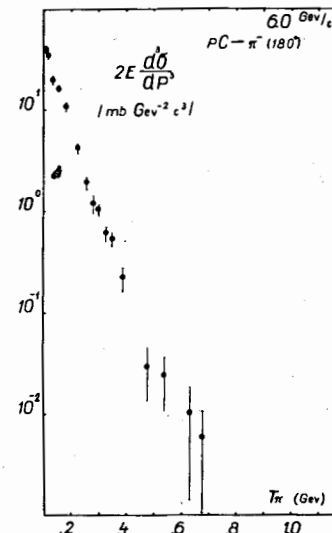


Fig. 2. Experimental data on the reaction $p + C \rightarrow \pi(180^\circ)$ for primary protons with momentum 6 GeV/c.

Fig. 3. Experimental data on the reaction $p + Al \rightarrow \bar{J}_1^-(180^\circ)$ for primary protons with momentum 6 GeV/c.

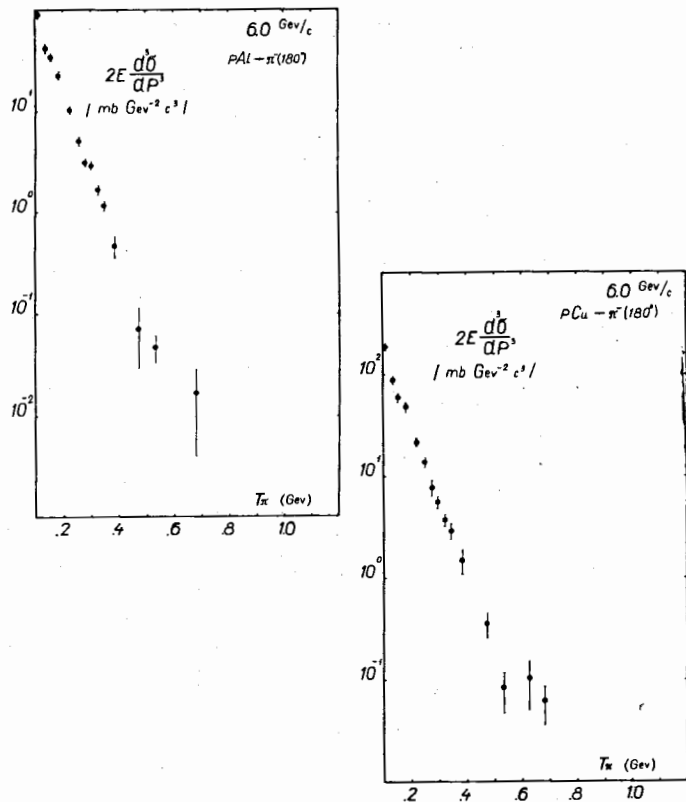


Fig. 4. Experimental data on the reaction $p + Cu \rightarrow \bar{J}_1^-(180^\circ)$ for primary protons with momentum 6 GeV/c.

Fig. 5. Experimental data on the reactions $p + C \rightarrow \bar{J}_1^+, K^+(180^\circ)$ for primary protons with momentum 8.4 GeV/c.

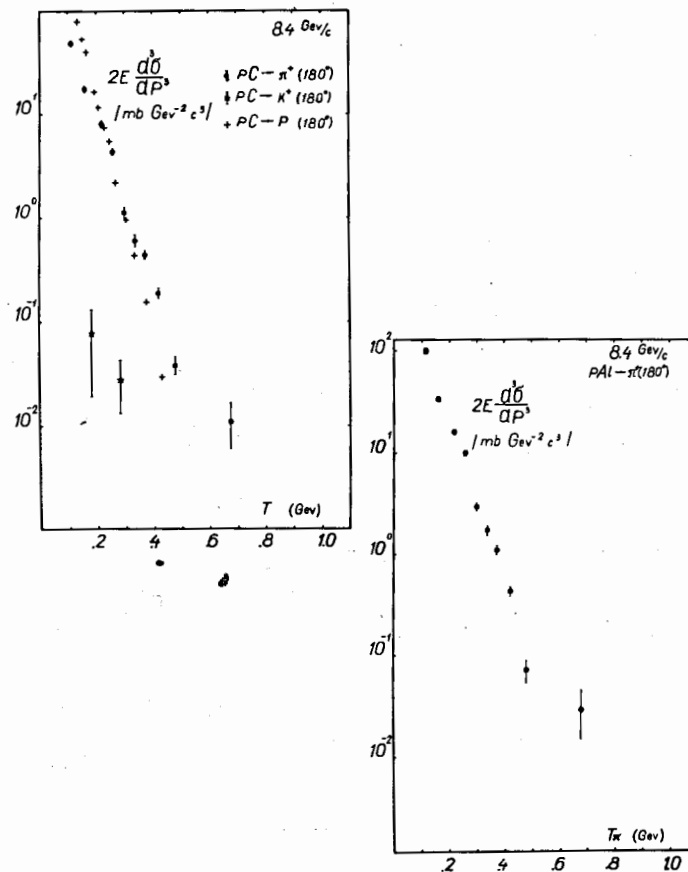


Fig. 6. Experimental data on the reaction $p + Al \rightarrow \bar{J}_1^+(180^\circ)$ for primary protons with momentum 8.4 GeV/c.

Fig. 7. Experimental data on the reaction $p + \text{Cu} \rightarrow J_1^+, k^+(180^\circ)$ for primary protons with momentum 8.4 GeV/c.

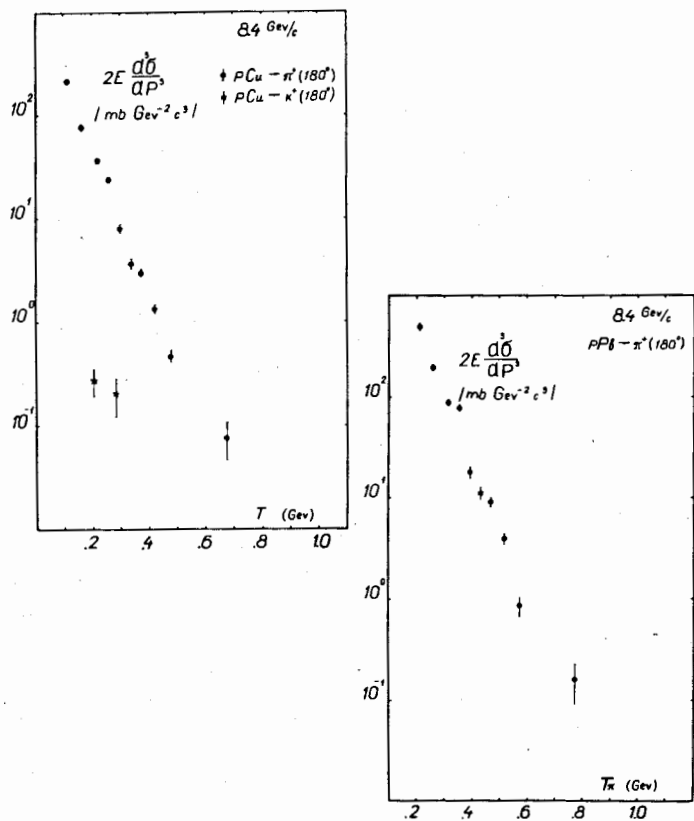


Fig. 8. Experimental data on the reaction $p + \text{Pb} \rightarrow J_1^+(180^\circ)$ for primary protons with momentum 8.4 GeV/c.

Fig. 9. Experimental data on the reaction $p + \text{C} \rightarrow J_1^-(180^\circ)$ for primary protons with momentum 8.4 GeV/c.

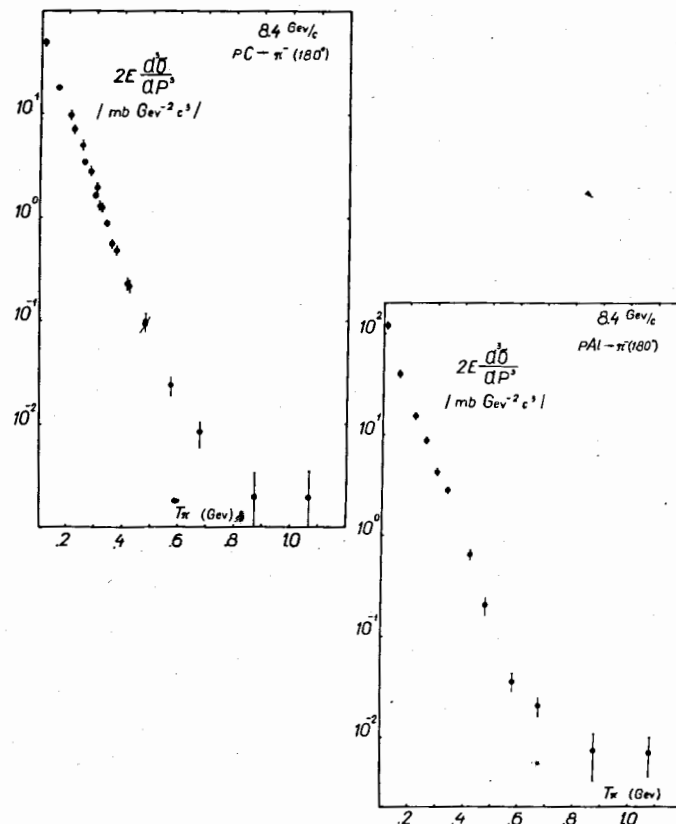


Fig. 10. Experimental data on the reaction $p + \text{Al} \rightarrow J_1^-(180^\circ)$ for primary protons with momentum 8.4 GeV/c.

Fig. 11. Experimental data on the reaction $p + \text{Cu} \rightarrow \pi^-$ (180°) for primary protons with momentum 8.4 GeV/c.

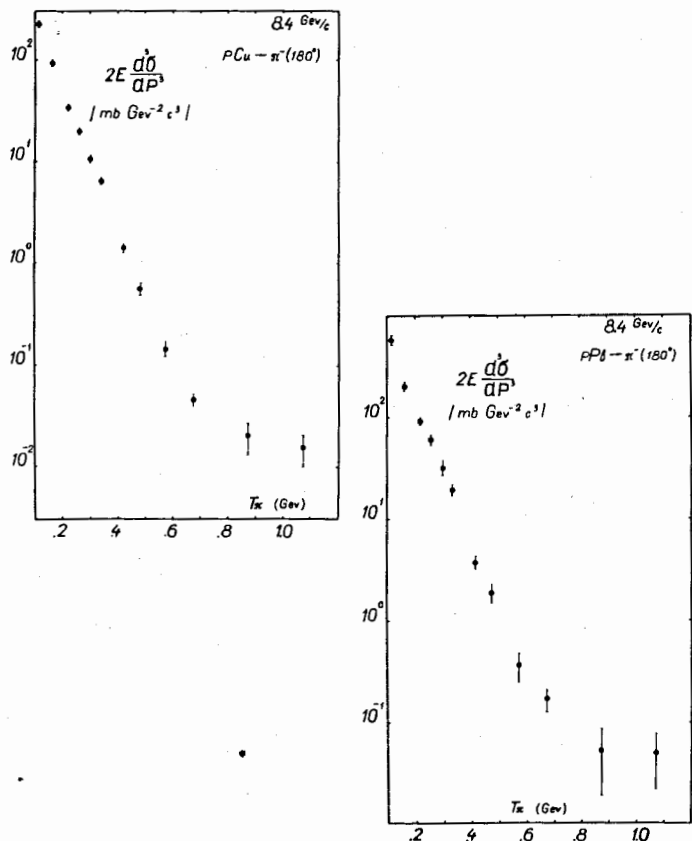


Fig. 12. Experimental data on the reaction $p + \text{Pb} \rightarrow \pi^-$ (180°) for primary protons with momentum 8.4 GeV/c.

Fig. 13. $2E d^3 \sigma / dp^3$ as a function of the atomic number for various energies of negative pions.

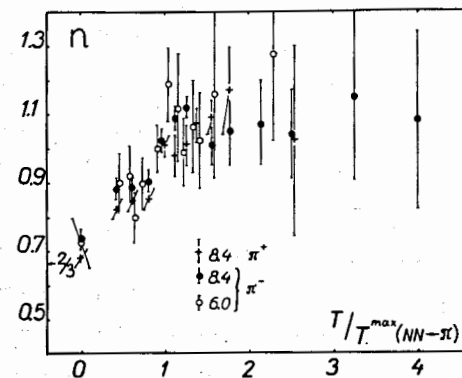
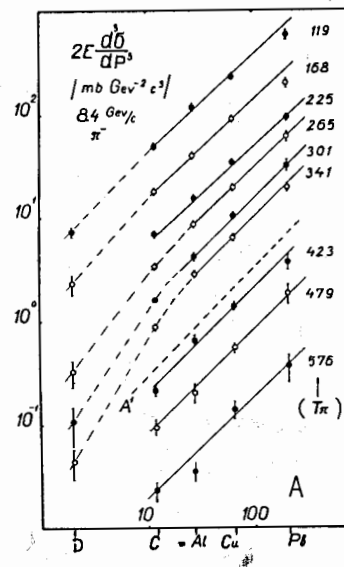


Fig. 14. $n (R_A = R_1 A)^n$ as a function of $\mathcal{E} = T / T^{\max}$.

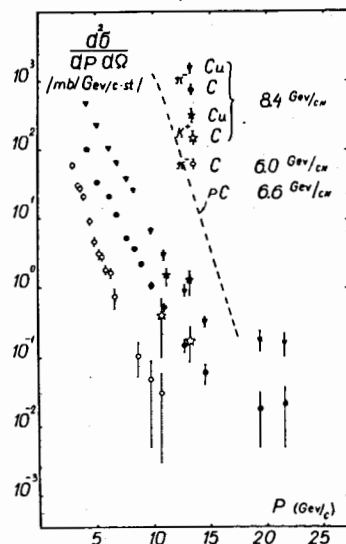


Fig. 15. Spectra of cumulatively produced particles.

References

1. A.M.Baldin, N.Ghiordanescu, V.N.Zubarev, A.D.Kirillov, V.A.Kuznetsov, N.S.Moroz, V.B.Radomanov, R.N.Ramzhin, V.A.Sviridov, V.S.Stavinsky, M.I.Yatsuta. JINR, PI-5819, Dubna, 1971.
2. A.M.Baldin, S.B.Gerasimov, N.Ghiordanescu, V.N.Zubarev, A.K.Ivanova, A.D.Kirillov, V.A.Kuznetsov, N.S.Moroz, V.B.Radomanov, V.N.Ramzhin, V.S.Stavinsky, M.I.Yatsuta. Yadernaya Fizika, v. 18, issue 1 (1973).
3. A.M.Baldin. JINR, P7-5769, Dubna, 1971.
4. A.M.Baldin. Brief Comm. on Physics No 1, AS USSR (1971), in Russian.

5. A.M.Baldin, N.Ghiordanescu, V.N.Zubarev, A.K.Ivanova, A.D.Kirillov, V.I.Kotov, N.S.Moroz, S.A.Nezhdanova, A.A.Povtorejko, A.D.Rogal, V.S.Stavinsky. JINR, I-8028, Dubna, 1974.
6. Yu.D.Bayukov, D.S.Vorobiev, G.P.Kartashov, G.A.Leksin, V.B.Fyodorov, V.D.Khovansky. Izv. Akad. Nauk SSSR, ser. fiz., v. 30, No 3, 521, 1966.
7. A.M.Baldin, Yu.D.Beznogikh, L.P.Zinoviev, I.B.Issinsky, G.S.Kazansky, A.I.Mikhailov, V.I.Moroz, N.I.Pavlov, G.P.Puchkov, JINR, P9-5442, Dubna, 1970.
8. H.H.Heckman, D.E.Greiner, P.J.Lindstrom, F.S.Bieser. Phys.Rev.Letters, 28, 926 (1972).
9. V.A.Alekseev, A.M.Baldin, Yu.D.Beznogikh, A.A.Vasiliev, M.A.Voevodin, E.I.Dyachkov, L.I.Zajdina, A.G.Zel'dovich, L.N.Zinoviev, I.B.Issinsky, G.S.Kazansky, I.F.Kolpakov, A.A.Kuzmin, L.G.Makarov, E.S.Mironov, A.I.Mikhailov, B.P.Murin, N.I.Pavlov, I.N.Semenyushkin, V.F.Sikolenko, A.A.Smirnov, V.D.Stepanyuk, A.P.Tsarenkov, K.V.Chekhlov. Comm. JINR, 9-7148, Dubna, 1973.
10. S.B.Gerasimov, N.Ghiordanescu. Comm. JINR, P2-7687, Dubna, 1974.

Received by Publishing Department
on June 28, 1974